THE JOURNAL OF PHYSICAL CHEMISTRY B

Article

pubs.acs.org/JPCB

Sensitivity of Water Dynamics to Biologically Significant Surfaces of Monomeric Insulin: Role of Topology and Electrostatic Interactions

Kushal Bagchi[†] and Susmita Roy*[,‡]

[†]St. Joseph's College for Arts and Science, Bangalore 560027, India

[‡]SSCU, Indian Institute of Science, Bangalore 560012, India

Supporting Information

ABSTRACT: In addition to the biologically active monomer of the protein insulin circulating in human blood, the molecule also exists in dimeric and hexameric forms that are used as storage. The insulin monomer contains two distinct surfaces, namely, the dimer forming surface (DFS) and the hexamer forming surface (HFS), that are specifically designed to facilitate the formation of the dimer and the hexamer, respectively. In order to characterize the structural and dynamical behavior of interfacial water molecules near these two surfaces (DFS and HFS), we performed atomistic molecular dynamics simulations of insulin with explicit water. Dynamical characterization reveals that the structural relaxation of the hydrogen bonds formed between the residues of DFS and the interfacial water molecules is faster than those formed between water and that of the HFS. Furthermore, the residence times of water molecules in the protein hydration layer for both the DFS and HFS are found to be significantly higher than those for some of the other proteins studied so far, such as HP-36 and lysozyme. In particular, we find that more structured water molecules, with higher residence times (∼300−500 ps), are present near HFS than those near DFS. A significant slowing down is observed in the decay of associated rotational auto time correlation functions of O−H bond vector of water in the vicinity of HFS. The surface topography and the arrangement of amino acid residues work together to organize the water molecules in the hydration layer in order to provide them with a preferred orientation. HFS having a large polar solvent accessible surface area and a convex extensive nonpolar region, drives the surrounding water molecules to acquire predominantly an outward H-atoms directed, clathrate-like structure. In contrast, near the DFS, the surrounding water molecules acquire an inward H-atoms directed orientation owing to the flat curvature of hydrophobic surface and the interrupted hydrophilic residual alignment. We have followed escape trajectory of several such quasi-bound water molecules from both the surfaces that reveal the significant differences between the two hydration layers.

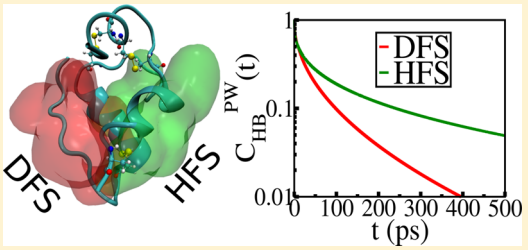

I. INTRODUCTION

The biologically active form of the protein insulin is a monomer consisting of two chains. One chain (called A-chain) is 21 amino acids long and the other (called B-chain) is 30 amino acids long. These two chains are linked by two disulfide bridges at A7-B7 and A20-B19. The A-chain also has an additional intrachain disulfide bond between A6 and A11. Insulin also exists, in its biologically inactive forms, as a dimer and a hexamer.[1] Although insulin receptor signaling has evolved to facilitate insulin binding only as a monomer to the insulin receptor, it ensures that this important protein is stored in the body as a dimer or hexamer.[2] However, insulin dimer, being relatively unstable, easily dissociates into monomers in blood circulation. The dimeric form, in turn, gets stabilized by the formation of the hexamer in the presence of zinc ions, during storage in the pancreatic β-cell.[3] So far several mutagenesis studies have generated different analogues of insulin to tune its pharmacokinetic properties by mutating on different potent sites on hexamer and dimer forming surfaces. In this process, insulin often yields the analogue with reduced ability of forming any bioaggregates.[3−5]

Water has a big role to play in insulin activity. It is known from numerous medical reports that *dehydration tends to raise blood sugar* and can cause temporary resistance to insulin causing "diabetes mellitus". It is a known fact that water intake can significantly stimulate the function and dynamics of insulin. It has been observed that plasma glucose decreased significantly in individuals after treatment with insulin and the time of the maximum decrease (30 min) was synchronized with the beginning of water intake.[6] Hence, there is a strong relationship between water and the function of insulin that is yet to be understood at a molecular level.

Despite extensive structural studies that have been done on insulin,[7−10] relatively little research has been focused on the molecular dynamics of water molecules around this protein or on dynamics of this protein in water. In 1991, Mark et al. studied the conformational flexibility of aqueous dimeric and monomeric insulin.[11] In 1999, Rossky and Cheng performed molecular dynamics simulations of 2-Zn insulin in water solvent

Received: November 12, 2013
Revised: March 17, 2014
Published: March 18, 2014

to investigate the effect of vicinal polar or charged groups on hydrophobic hydration at a biomolecular surface.[12] In the same year, Chai and Jhon performed molecular dynamics study on interfacial hydration structure surrounding insulin molecule at high pressure.[13] While the water structure around insulin has been studied by Chai and Jhon, and Badger and Caspar,[13,14] to the best of our knowledge, no prior study exists that has evaluated the *dynamics of interfacial water* surrounding insulin and the connecting role of such "biological water" with the structural morphology of the two distinct surfaces of insulin.

It has been known for a considerable amount of time that water in confined systems (like reverse micelles and nanotubes) and in biomolecular hydration layer exhibits properties different from those of bulk water.[15−21] Water in the protein hydration layer shows restricted motion in comparison to the free movement of molecules of bulk water.[22−27] Such water molecules not only are important for the thermodynamic stability of the proteins and DNA, but also play a central role in several biomolecular functions, such as intercalation, catalysis, recognition, and so forth. An example is provided by adenylate kinase (ADK) where water molecules help in stabilizing a half-open-half-closed (HOHC) state that further facilitates substrate capture subsequent to product release.[28] Quasi-bound water molecules in the binding pocket of protein play a crucial role in noncovalent association of proteins and small drug compounds. The interaction between the binding site of protein and drug molecules depends upon the release of these bound water molecules.[29,30]

The heterogeneity of an amphiphilic protein surface extends from largely hydrophobic to largely hydrophilic. While water molecules are usually found to form stable H-bonding network near hydrophilic residues through electrostatic interaction,[31−33] the vicinal hydrophobic patches often intervene.[34−38]

In a pioneering study, Rossky and co-workers have elucidated the effect of surface topography on the interfacial solvent structure in their numerous studies. They reported that the hydration of extended nonpolar planar surfaces that often appears to involve in structures is orientationally inverted in contrast to the clathrate-like hydration shell. While the clathrate-like structures predominate near convex surface patches, a dynamic equilibrium exists between clathrate-like and less-ordered, inverted water structures in the hydration shell near flat surfaces.[39,40] In a subsequent work, they have explored the effect of vicinal polar and charged groups on hydrophobic hydration. In addition, they have compared the structural orientations of water molecules around 2-Zn insulin and melittin dimeric surfaces. The dimer forming surface of insulin is largely flat except with a slight curved exposure of Phe-25. Further, the presence of vicinal polar residues causes substantial fluctuation to such hydration structure.[41]

Dimer forming surface (DFS) and hexamer forming surface (HFS) both are nonpolar.[42] While DFS is flat and aromatic in nature, the other surface is more extensively nonpolar and convex. The DFS surface is buried upon insulin dimer formation, and HFS is buried when dimers assemble to form hexamer. The DFS of insulin is collectively hydrophobic (effective hydrophobicity 1.4, according to hydropathy scale) blended with a large number of hydrophilic amino acids. DFS contains B8 Gly, B9 Ser, B12 Val, B13 Glu, B16 Tyr, B23 Gly, B24 Phe, B25 Phe, B26 Tyr, and B27 Thr. Nevertheless, the presence of residues like B12 Val, B24 Phe, and B25 Phe, being extensively hydrophobic in nature, plays very important role in the dimer link formation. The HFS of insulin is also largely hydrophobic (effective hydrophobicity 10.9, according to hydropathy scale) made of amino acids B1 Phe, B2 Val, B4 Gln, B13 Glu, B14 Ala, B17 Leu, B18 Val, B19 Cys, B20 Gly, A13 Leu, A14 Tyr, and A17 Glu. This should explain, qualitatively, the weak stability of an insulin dimer that is associated with a small hydrophobic area and the enhanced stability of an insulin hexamer that is associated with a large hydrophobic patch.

We organize the rest of the Article as follows. In the next section, we briefly describe the system studied (insulin and water) and the simulation details. Section III contains the dynamical characterization of water near DFS and HFS of insulin. Section IV involves the correlation between structure and dynamics. Section V concludes with a brief summary of results.

II. STRUCTURAL DETAILS OF THE PROTEIN STUDIED AND SIMULATION SETUP

The monomer of insulin is composed of two polypeptide chains, namely A-chain and B-chain. A chain involves 21 amino acid residues and B chain consists of 30 amino acid residues (see Figure 1). These two chains are interlinked though a

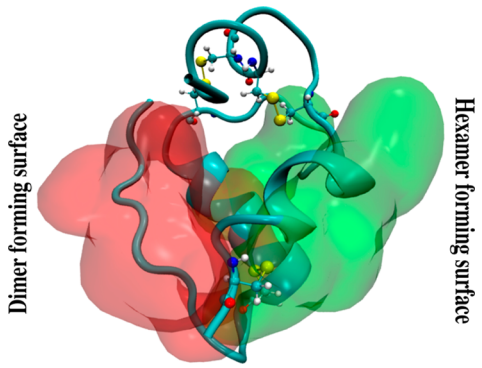

Figure 1. Ribbon based surface diagram showing two different surfaces of an insulin molecule, with the red color for dimer forming surface (DFS) and the green one for hexamer forming surface (HFS). One insulin molecule is made of two chains: A-chain and B-chain. These two chains are interconnected through two disulfide bridges formed between A7−B7 and A20−B19. There is an intrachain SS-bridge also formed between A7 and A11. The location of these three disulfide bonds those are essential for insulin-receptor binding process and also in stabilizing the secondary structure are shown in the figure.

disulfide bridge formed between A7−B7 and A20−B19. In addition, A-chain has an intrachain SS-bridge formed between A7 and A11. All these three disulfide bonds are essential for the receptor binding activity of insulin, as well as to preserve its secondary structural integrity. Even among different species, these three disulfide links along with certain amino acid sequences remain highly conserved.[10] Such similarities in secondary structure rendering equivalent biological efficiency among different species have often been utilized for medication. As for example, pig insulin is widely exploited in human patients for medical treatment.

To assess the dynamics of insulin we performed molecular dynamics (MD) simulations of the protein in explicit water by using the Groningen Machine for Chemical Simulation (GROMACS Package). The simulation began with the crystal structure of the pig insulin monomer.[43] The initial coordinate was collected from the Protein Data Bank (PDB-ID: 9INS). All

dx.doi.org/10.1021/jp411136w | J. Phys. Chem. B 2014, 118, 3805−3813

atom topologies were generated with the help of pdb2gmx. We have applied the tricks of merging the two chains (A and B) and preserved the interchain disulfide linkage. We have treated the system with OPLS set of parameters available in GROMACS. Initially protein is centered in a cubic box with length of 5.25 nm. Then insulin monomer was solvated with pre-equilibrated SPC/E water model using genbox.[44] A total of 4534 water molecules were added. After steepest descent energy minimization, each trajectory was propagated in an NVT ensemble and equilibrated for 2 ns. All the simulations in this study were done at 300 K and 1 bar pressure. The temperature was kept constant using the Nose−Hoover thermostat.[45,46] It was followed by an NPT equilibration for 20 ns using the Parinello−Rahman barostat for production run.[47] Each simulation used a time-step of 2 fs. All the analyses were executed from the equilibrated trajectory by excluding first 15 ns time steps. However, for dynamical characterization, we have saved the equilibrated trajectory with a 2 fs time resolution. Periodic boundary conditions were applied and nonbonded force calculations employed with a grid system for neighbor searching. Neighbor list generation was performed after every 1 step. A cutoff radius of 1.0 nm was used both for neighbor list and van der Waals' interaction. To calculate the electrostatic interactions, we used PME[48] with a grid spacing of 0.12 nm and an interpolation order of 4.[49]

III. RESULTS: DYNAMICAL VARIATION

A. Reorientational Dynamics of Surface Water. Although a tentative picture of water arrangement around the surfaces of different proteins have emerged in recent years, no detailed study of water dynamics surrounding insulin seems to exist. The reorientational dynamics of water molecules near the heterogeneous macromolecular surfaces (such as protein, DNA, etc.) is known to be significantly affected.[50] The reorientational motion of water can be evaluated by measuring the average time autocorrelation functions $C_i(t)$ of any bond vector i. The time correlation function (TCF) is defined as

$$C_i(t) = \frac{\langle \hat{e}_i(t+\tau)\, \hat{e}_i(\tau)\rangle}{\langle \hat{e}_i(\tau)\, \hat{e}_i(\tau)\rangle} \quad (1)$$

Here $\hat{e}_i(t)$ is the unit vector of the corresponding bond at time, t.

To investigate the dynamical behavior of water molecules near both HSF and DFS of insulin, we evaluate the reorientational motion of the water molecules that are in the proximity to those surfaces (i.e., within 4.2 Å from the atoms of individual surfaces). The correlation functions were calculated by averaging over these water molecules only. In Figure 2 we show the variation of $C_{O-H}(t)$ against time for water molecules near those surfaces. For comparison, we have also plotted the relaxation for the bulk water. Note the significant slowing down of rotational motion of water molecules in the insulin hydration layer when it is compared with that of the bulk water. Again, it is clearly evident from the figure that the water molecules around DFS reorient noticeably faster than those around HFS which signifies that the hydration layer near DFS is less ordered. In addition, the evidence of faster reorientational motion of water near DFS correlates well with the fact of less stable dimer formation than more stable hexamer.

Study of mean square deviation (MSD) of water molecules near the surfaces, namely, DFS and HFS, also indicates that the

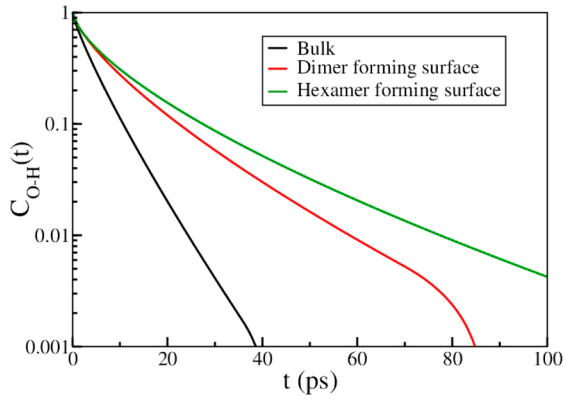

Figure 2. Time evolution of reorientational time correlation function (TCF) of the O−H bond vector of water molecules near the two biologically significant surfaces of insulin. The red curve shows the decay of TCF near the DFS, while the green curve shows the decay of TCF near the HFS. The TCF for the water molecules present in the bulk (black curve) is also presented for comparison. Note the slow dynamics in relaxation of TCFs both near DFS and HSF. However, the emergence of long time tail for water TCF near HFS is noticeable.

DFS hydration layer shows comparatively faster dynamics than that around the HFS.

Furthermore, to understand the observed time correlation functions in a more quantitative way, we have estimated the time scales associated with those quasi-bound water molecules located next to both surfaces. We notice that even though the water molecules around DFS reorient more quickly compared to those around HFS, all the curves show slower decay at longer times. Such long-time decay cannot be described by a single-exponential law. Here we observe that the computed TCFs are best fitted by stretched exponential functions of time with stretching exponents (β) in the range of 0.6−0.8 that provides reasonable fits of the data. The expression used for the best fit is as follows:

$$C_{O-H}(t) = e^{-(t/\tau)^{\beta}} \quad (2)$$

The parameters for the best fit are shown in Table 1.

Table 1. Stretched Exponential Fitting Parameters for the Reorientational Time Correlation Functions of Interfacial Water Molecules around the DFS and HFS of Insulin Also in Comparison with Bulk

	τ (ps)	β	$\langle\tau\rangle$ (ps)
bulk	3.95	0.84	4.32
DFS	7.0489	0.71	8.64
HFS	7.879	0.6347	10.41

In general, the values of β often endow with a significant nonexponential nature to the time correlation functions. It is often conjectured that such nonexponential dynamics reflect the non-Markovian character of rotational friction in *slowly relaxing solvents*, like ionic liquids. Subsequently, this non-exponentiality often bears the characteristics of dynamical heterogeneity in the solution.[51]

It is clear that the water molecules around HFS exhibit significantly slower dynamics with a long time component. In the recent past, similar slow decay has also been observed in a number of related studies for proteins, like HP-36 and enterotoxin.[52,53] As discussed above, the existence of such a

dx.doi.org/10.1021/jp411136w | J. Phys. Chem. B 2014, 118, 3805−3813

long time component arises because of some particular water molecules that are "quasi-bound" to some specific residues on protein surfaces. The present result and estimated time scales clearly suggest that even though the rotational motion of water at the interface of a protein is much slower compared to that of bulk water, significant difference in water motion might arise due to the distinct topographical nature of insulin surfaces. Such diverse structural characteristics of protein surfaces may have an immense influence over the dynamics of surrounding water molecules and also over the binding activity of a protein molecule. To obtain a microscopic understanding of these phenomena, it would be interesting to study the hydrogen bond forming affinity of water molecules with the adjacent protein residues.

B. Hydrogen Bond Lifetime Kinetics in the Two Layers. Depending on the number and nature of hydrogen bonds (H-bonds) that these water molecules make with the charged/polar amino acid residues on the protein surface, we can divide them broadly into two classes: (i) interfacial quasi-bound water and (ii) interfacial free water.[53] These interfacial free water molecules do not form any hydrogen bonds with the protein residues whereas interfacial quasi-bound water molecules might exist in either singly or doubly hydrogen bonded form. Interfacial free water molecules, of course form hydrogen bonds with neighboring water molecules and experience van der Waals' type interactions with protein atoms if they are within the range of any sort of interaction potential.[54,55] One can use either a geometric or an energetic criterion to define a hydrogen bond. In the present work, we have applied solely the geometric criterion to define a hydrogen bond.[50]

The structural relaxation of water molecules in terms of hydrogen bonds can be expressed as

$$C_{HB}(t) = \frac{\langle h(t+\tau)\, h(\tau)\rangle}{\langle h\rangle} \qquad (3)$$

According to the definition the hydrogen bond population variable, $h(t)$ is unity when a particular pair of protein−water or water−water sites is hydrogen-bonded at time t and is zero otherwise.[56−59] The angular brackets denote averaging over all protein−water hydrogen bonds and over initial time τ. Here we have not presented the water−water hydrogen bond dynamics. The correlation function $C_{HB}(t)$ allows the reformation of a bond that was broken at some intermediate time. In fact, it allows recrossing the barrier separated hydrogen bonded and nonbonded states. Thus, the relaxation of $C_{HB}(t)$ offers the information about the structural relaxation of a particular hydrogen bond. The computed hydrogen bond TCFs are best fitted by stretched exponential functions of time with stretching exponents (β) in the range of 0.35−0.50 that provides reasonable fits of the data. The parameters for best fit are shown in Table 2. In the present, case we have evaluated hydrogen bond time correlation function for water molecules those are specifically close to either DFS or HFS (see Figure 3a for $C_{HB}(t)$). Both reorientational and hydrogen bond time correlation function calculations were carried out from the simulation trajectories with the time resolution of 2 fs.

Table 2. Stretched Exponential Fitting Parameters for the Hydrogen Bond Time Correlation Functions of Interfacial Water Molecules around the DFS and HFS of Insulin

	τ (ps)	β	$\langle\tau\rangle$ (ps)
DFS	18.372	0.497	35.295
HFS	24.9374	0.368	69.305

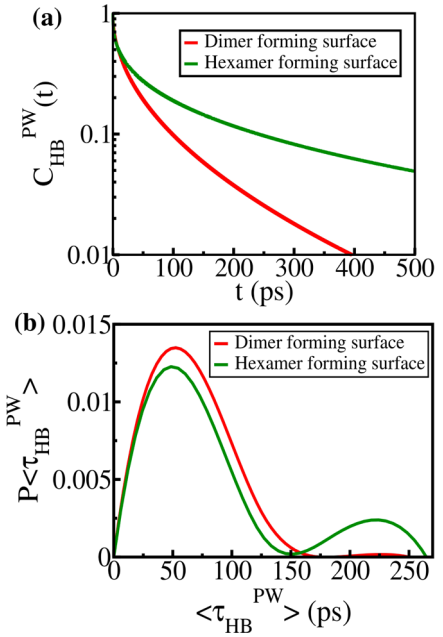

Figure 3. (a) Hydrogen bond lifetime dynamics of water molecules near the two surfaces: DSF (red) and HFS (green). Note the slower hydrogen bond relaxation behavior near HFS. (b) Distribution of H-bond lifetime ($P < \tau_{HB}^{PW}>$) near DFS and HFS. H-bonds near DFS are characterized by a broad range of distribution. Distribution of H-bond lifetime near HFS is bimodal. The second peak is associated with large H-bond survivals.

While the most interesting observation we found is the significant difference in the relaxation behavior of hydrogen bond dynamics between DFS−water H-bonds and HFS−water H-bonds, more detailed information is provided by the distribution of H-bond lifetime associated with individual molecules of the protein surface (see Figure 3b). Such distribution is a wonderful showcase which illustrates a broad range of heterogeneity that extends throughout the protein surface. Though the H-bond lifetime distribution near DFS is however associated with a large standard deviation, the same near HFS shows a clear bimodal distribution with a second peak ranged between 150 and 250 ps. Thus, similar as in the above figure, we again find the structural relaxation of the protein−water hydrogen bonds is much slower for HFS than that of DFS. These results also correlate well with the biological functionality of the protein because most of the hydrophobic residues of insulin are congregated in HFS to form the stable hexamer.

C. Residence Time Distribution of Hydration Water. The slow dynamical behavior of water near HFS and DFS provides the signature of the presence of a number of quasi-bound water molecules that are motionally restricted at the insulin surfaces. To distinguish the propensity and survival time of such quasi-bound water molecules in the hydration layer, we evaluate their residence time distribution, shown in Figure 4. The residence time distributions, for both the hexamer and dimer forming surface, peak at around 150 ps which is unexpectedly high. This indicates the entire hydration layer structured to a certain extent. Such a long residence time has

dx.doi.org/10.1021/jp411136w | J. Phys. Chem. B 2014, 118, 3805−3813

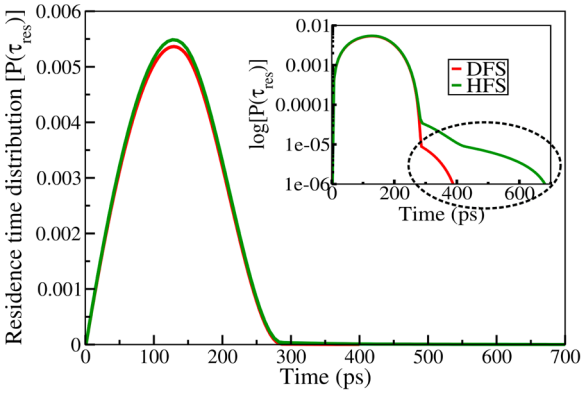

Figure 4. Residence time distribution near the DFS and HFS surfaces. The color code is the same as in the previous figures. Logarithm of residence time distribution captures those water molecules that stay in the hydration layer more than 200 ps. In the inset of the figure, they are highlighted by black dotted circle. Note the long time tail in the residence time distribution of water molecules near HFS.

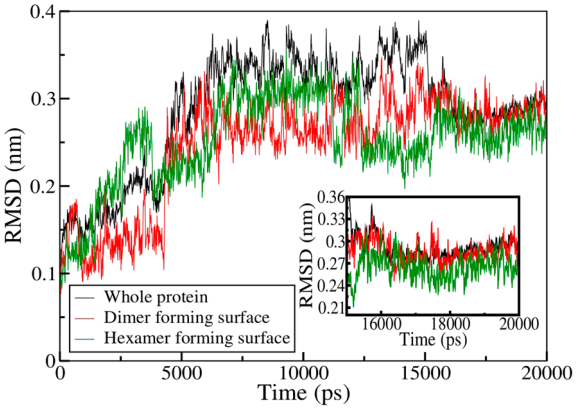

Figure 5. Time dependence of the RMSD of the whole protein (shown in black), the DFS (shown in red), and the HFS (shown in green). The equilibrium RMSDs for the two surfaces are highlighted from 15 000 ps to 20 000 ps in the inset which shows remarkable lowering of the RMSD of HFS. The higher RMSD values for DFS residues indicate a more flexible environment around that specific region.

not been observed in other similar studies such as those with HP-36.[53]

A curious phenomenon is observed for the water molecules around the hexamer forming surface. Some water molecules have even a residence time extending to 700 ps which is unusually high. These water molecules are found to be mostly either singly, doubly or triply hydrogen bonded to the protein residues. The population of such water molecules is never large but non-negligible near the HFS. But a much larger population in the more mobile (low residence time) region (less than 150 ps) may suppress the contribution from those "slow" interfacial water molecules which are less in number but more strongly bound to the protein surface. To separate out exceptionally strongly bound water molecules we have shown the logarithmic scale of residence time distribution. It captures those water molecules that reside more than 200 ps as shown in the inset of Figure 4. In this inset plot, a clear appearance of the long time tail in residence time distribution near HFS illustrates that there exists a fraction of water molecules with residence time in the range of 400−700 ps. The number of such quasi-bound water molecules with long survival time is indeed very small.

IV. CORRELATION BETWEEN STRUCTURE AND DYNAMICS

A. RMSD. To understand the dynamical coupling between the conformational fluctuation of protein and surrounding water molecules, we have monitored the root-mean-square deviation (RMSD) of position of all non-hydrogen atoms involved in the whole protein, particularly those involved in forming the DFS and the HFS. This is shown in Figure 5. RMSD often provides key information about the side chain mobility of the residues which can influence and also be influenced by the hydration layer dynamics. It is interesting to note that highly hydrophobic hexamer forming surface has a lower root-mean-square deviation, on the whole, which implies that it is more rigid than the dimer forming surface or than the whole protein. Such rigidity assists in building up a stable hydration layer in the HFS premises. There are several reports suggesting that protein dynamics is controlled by the water dynamics. The present result indeed is a good example of the same.

B. Correlation Of Water Dynamics with Effective Hydropathy Index and SASA. The hexamer forming surface consists mostly of highly or moderately hydrophobic residues: Phe(B1), Val B2, Ala(B14), Leu(A13 andB17), Val(B18), Cys(B19). Others are hydrophilic at neutral pH: Gln (B4) and Glu (B13 and B17), Gly (B20) and Tyr (A14). The hexamer forming surface has a higher, relatively nonpolar, significantly exposed and extended convex hydrophobic solvent accessible surface area (see Table 3). In contrast, the dimer forming surface involves less number of hydrophobic residues, namely, Val (B12), Phe (B24 and 25), Leu (A13 and B17), and more hydrophilic residues, such as Ser (B9), Glu (B13), Tyr (B16 and 26), and Thr (B27) along with Gly at B8 and B23 positions. Thus, a higher polar solvent accessible surface area of DFS is expected. Following the hydropathy scale index, we have calculated an effective hydropathy index considering all the involved residues along both surfaces. It provides an intuitive idea to understand and explain the events of a specific surface. This hydropathy estimate shows that while DFS has an overall hydrophilic index −8.4, HFS has overall hydrophilic index −12.2. More interestingly, while DFS has overall hydrophobic index 9.8, HFS has overall hydrophobic index 23.2. Thus, HFS with elevated hydrophilic and hydrophobic character might be responsible for observed dynamical retardation.

Table 3. Estimation of Effective Hydropathy Index, In Terms of Overall Hydrophilicity and Overall Hydrophobicity Following the Hydropathy Scale[a]

surface	overall hydrophilicity	overall hydrophobicity	polar SASA	nonpolar SASA
DFS	−8.4	9.8	28.8%	71%
HFS	−12.2	23.1	35.9%	63.1%

[a]In comparison, the evaluation of relative polar and nonpolar SASA (solvent accessible surface area) of DFS and HFS is also indicated in the table.

Other than the hydropathy estimates, the relative exposure of the polar probe residues in different surfaces might play a role which determines the essential part of protein−water interaction causing such slow dynamics. To estimate the

dx.doi.org/10.1021/jp411136w | J. Phys. Chem. B 2014, 118, 3805−3813

exposure of the polar probe we have calculated relative polar solvent accessible surface area averaged over 20 ns trajectory (shown in Table 3). We find that the solvent accessibility to the polar probe is low near DFS (28.8%) compared to that of HFS (35.9%). Despite the presence of extended hydrophobic surface we have observed that HFS is designed in such a way that polar residues are next to another polar neighbor that assists to bind the water molecules near HFS.

C. Role of Protein−Water Electrostatic Interaction Energy. The time evolution of protein-water electrostatic interaction energy per residue for both DFS and HFS are shown in Figure 6. The figure shows that the quasi-bound water

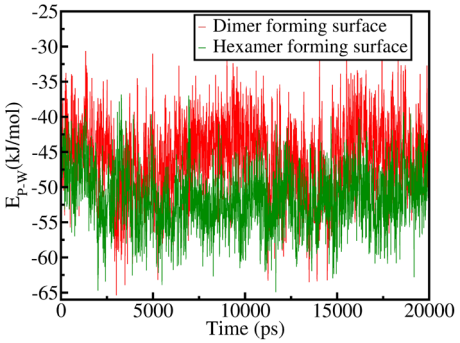

Figure 6. Time progression of protein−water electrostatic interaction energy per residue. Comparison between the relative electrostatic interaction energy for DFS and HFS clearly shows the higher stability of HFS hydration layer.

molecules near HFS are displaying higher stability with more negative interaction potential. Such quasi-bound water molecules are stabilized by about 20 kJ/mol energy compared to DFS. It mostly arises due to the abundance of doubly hydrogen bonded water molecules near HFS and their strong electrostatic interaction with the protein residues. However, these quasi-bound water molecules have lower entropy which is found to play an important role in determining their overall stability.

D. Quasi-bound Water Crowding near DFS and HFS. We detect a few motionally restricted water molecules located near HFS that are doubly hydrogen bonded to the protein residues. When we extracted several snapshots from simulation trajectory, we observed that a large number of water molecules with high survival time are crowded near HFS. In Figure 7, we show such a cluster of water molecules that are captured in one snap. In comparison to HFS, a lesser number of water assemblies is found near DFS (see Figure 7). The higher residence time of the HFS may be attributed to the presence of an exposed hydrophilic residues (B4 Gln, B13 Glu, A14 Tyr, and A17 Glu), in combination with the presence of a largely hydrophobic surface which restricts the options to avail that unfavorable surface. The encaged water molecules thus revolve around that hydrophobic area for a long time and thus account for the unusually high residence time in the hydration layer. On the contrary, the hydrophilic groups that are involved in DFS are mostly located between two hydrophobic shells of DFS and HFS. Such hydrophilic residues those are located in the intersection of two extended hydrophobic region themselves exhibit large fluctuations in position rendering the location unstable (or unsuitable) for water.

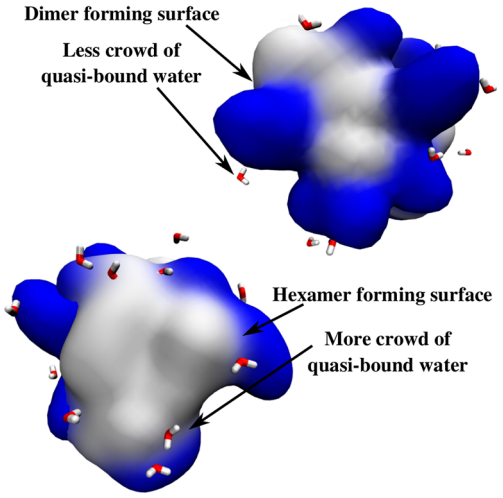

Figure 7. Representative snaps extracted from the simulation trajectory, showing the location of several water molecules adjacent to the surfaces of DFS (upper) and HFS (lower). The number of quasi-bound water molecules attached to the dimer forming surface is less than the number bound to the hexamer forming surface. Note that quasi-bound water channel around the extensive hydrophobic surface of HFS.

Although the hydrophilic residues and their spatial arrangement induce the water molecules to stay in the hydration layer through electrostatic interaction, the aversion of extended hydrophobic patch is also believed to play a role in their stay in the hydration shell. To address the surface topographical dependence of hydrophobic hydration (by the proximal water molecules) we have looked into the water orientation along the protein surface. We find the result somewhat similar to the observations by Rossky and co-workers.[40] In this analysis, we consider the vector of water dipole pointing outward from the central oxygen atom as it can form four hydrogen bonds. Now we measure the angle (θ) between the vector of this resultant dipole and tangential vector associated with the protein surface normal and oxygen of water. See Figure 8 for an illustration. The probabilistic distribution of cosine angle reflects the structure of the hydration shell. We find that the distribution maximizes sharply near −1 and 1 that are belonging to outward H-atoms directed (clathrate-like) hydration shell and inward H-atoms directed (inverted-like) respectively. Additionally, we observe two broad maxima appear over the range of −0.33 to −0.42 near inward H-atoms directed region and on the other side over the range of 0.33 to 0.50 near outward H-atoms directed hydration shell. These values might correspond to the other connected hydrogen bonds that are spatially form tetrahedral arrangements. In a previous study Rossky et al. has detected similar values in such distribution.[40]

The investigation of water orientation correlates well with the topographical construct of the corresponding hydrophobic surface of DFS and HFS. In DFS, the residues are arranged in a flat surface.[43] Although in DFS, Phe (B25) being more convex and exposed prefers a clathrate-like hydration arrangement, Phe (B24), Val (B12) residues prefer an inverted-like hydration shell due to the influence of adjacent polar residues such as Arg (22) and Glu (B13) respectively. In HFS, while a large number of residues are exposed, such as Phe(B1), Val (B2), Leu (A13 andB17), and Val (B18), two residues, Ala (B14) and Cys(B19), are found to be buried. However, a large hydrophilic surface exposure and highly convex restricted hydrophobic area

dx.doi.org/10.1021/jp411136w | J. Phys. Chem. B 2014, 118, 3805−3813

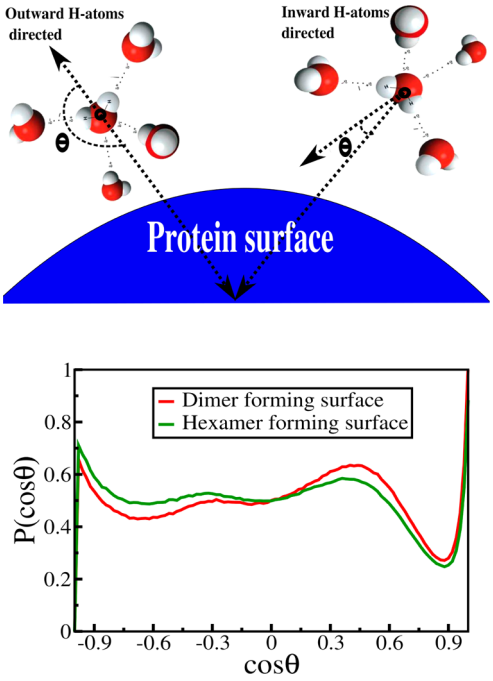

Figure 8. Orientational distribution of water molecules in the hydration shell relative to the normal of the protein surface. Upper panel provides a pictorial description of the angle θ, between the vector of water dipole and the protein interface. θ categorizes water molecules into one of the two forms: (i) either outward H-atoms directed arrangement if cos θ value is near −1 or (ii) inward H-atoms directed arrangement if cos θ value is 1. A broad maximum appears over the range of −0.33 to −0.42 which corresponds to the orientation of those water molecule that are connected outward with an inward H-atoms directed water molecule. On the other hand, over the range of 0.33−0.50, another broad maximum appear which corresponds to the orientation of those water molecule that are tetrahedrally linked inward with an outward H-atoms directed water molecule in the hydration shell.[40]

consent to the hydration shell to slightly shift toward more ordered outward H-atoms directed distribution.

V. CONCLUSION

Given the paramount importance of water in the biological function of insulin, it is interesting to find the substantial differences in the solvation characteristics of the two surfaces of an insulin molecule. The observed differences could have important consequences in dimerization and aggregation of these protein molecules. We have obtained several potentially important results. First, the residence times of water molecules in the protein hydration layer for both the DFS and HFS are found to be significantly higher than those known for some other proteins that have been studied so far, such as HP-36 and lysozyme. Crystallographic studies have also identified the presence of such structurally ordered water molecule in insulin hydration layer.[60] In particular, we find that more structured water molecules, with higher residence times (∼300−500 ps), are present near HFS than those near DFS. Second, dynamical characterization reveals that kinetics of the hydrogen bonds formed between the residues of DFS and the interfacial water molecules are faster than that formed between water and the HFS. Third, a significant slowing down is observed in the decay of associated rotational auto time correlation functions of O−H bond vector of water in the vicinity of HFS.

The dynamical behavior of interfacial water molecules is complex and often defies any generalization. There are several views on the complex movement of hydration layer water molecules depending on protein surface topography. In the recent past, the hydration structure of human lysozyme was analyzed by using molecular dynamics simulations by Jana et al., and several similar reports also exist associated with other proteins.[24,32,50] These studies found both fast water motion and stable hydrogen bonding (H-bond) network near hydrophilic patches, reflecting the role of electrostatic interaction between the polar amino acid residues. Several studies have also revealed structural ordering of water molecules near hydrophobic surfaces.

In the present case, the reason behind distinct dynamical behavior cannot be attributed solely to the hydrophilic−hydrophobic proportion but due attention should be given also to their length scale and relative arrangement of the groups. The HFS, so designed, has a large hydrophilic exposure blended with an extensively restricted hydrophobic convex area. Thus, the water molecules that are strongly hydrogen bonded to the hydrophilic residues of HFS become more constrained and structured. The hydrophilic residual alignment also providing cooperativity to the adjacent polar group assists to build a stable water channel surrounding the reviled hydrophobic area. The convex nonpolar residues all along restricting the water motion direct them to orient in an outward H-atoms directed, clathrate-like arrangement. The dynamical slowing down in HFS is attributed to such ordering in the hydration structure.

However, in the case of DFS, the hydrophilic residues are often interrupted by the intervening hydrophobic moieties. Such interventions lead a fluctuating hydration shell around DFS. In addition, a large portion of DFS hydrophobic surface is flat. Such topography directs the vicinal water molecule to orient in an inverted arrangement. Thus, the highly fluctuating protein dynamics near DFS leads the hydration structure to be less structured, and therefore, we obtain a relatively fast water dynamics in DFS hydration shell.

Water molecules near DFS experience smaller free energy barrier height that separates them from the bulk water. We have traced the trajectory of several such quasi-bound water molecules from both surfaces toward their escape into the bulk (see Figure S1 in the Supporting Information). The "slow" water molecules may play an important role in stabilizing hexamer forming surface of the protein and, thus, perhaps, assist in the formation of stable bioassembly. This aspect deserves further study.

■ ASSOCIATED CONTENT

Ⓢ Supporting Information

Details of quasi-bound water motion in the insulin hydration layer. This material is available free of charge via the Internet at http://pubs.acs.org.

■ AUTHOR INFORMATION

Notes

The authors declare no competing financial interest.

■ ACKNOWLEDGMENTS

This work was supported by grants from DST, India. We thank Prof. B. Bagchi for many useful discussions.

REFERENCES

(1) Baker, E. N.; Blundell, T. L.; Cutfield, J. F.; Cutfield, S. M.; Dodson, E. J.; Dodson, G. G.; Hodgkin, D. M. C.; Hubbard, R. E.; Isaacs, N. W.; Reynolds, C. D.; et al. The Structure of 2ZN Pig Insulin Crystals at 1.5Å Resolution. *Philos. Trans. R. Soc. London, Ser. B* **1988**, *319*, 369−456.

(2) Steiner, D. F. The Banting Memorial Lecture 1976. Insulin Today. *Diabetes* **1977**, *26*, 322−340.

(3) Dodson, G.; Steiner, D. The Role of Assembly in Insulin's Biosynthesis. *Curr. Opin. Struct. Biol.* **1998**, *8*, 189−194.

(4) Quinn, D.; Orci, L.; Ravazzola, M.; Moore, H. P. Intracellular Transport and Sorting of Mutant Human ProInsulins That Fail to Form Hexamers. *J. Cell Biol.* **1991**, *113*, 987−996.

(5) Shoelson, S. E.; Lu, Z. X.; Parlautan, L.; Lynch, C. S.; Weiss, M. A. Mutations at the Dimer, Hexamer, and Receptor-Binding Surfaces of Insulin Independently Affect Insulin-Insulin and Insulin-Receptor Interactions. *Biochemistry* **1992**, *31*, 1757−1767.

(6) Vijande, M.; Lopez-Sela, P.; Brime, J. I.; Bernardo, R.; Diaz, F.; Costales, M.; Marin, B. Insulin Stimulation of Water Intake in Humans. *Appetite* **1990**, *15*, 81−87.

(7) Bentley, G.; Dodson, E.; Dodson, G.; Hodgkin, D.; Mercola, D. Structure of Insulin in 4-Zinc Insulin. *Nature* **1976**, *261*, 166−168.

(8) Zoete, V.; Meuwly, M.; Karplus, M. A. Comparison of the Dynamic Behavior of Monomeric and Dimeric Insulin Shows Structural Rearrangements in the Active Monomer. *J. Mol. Biol.* **2004**, *342*, 913−929.

(9) Schlitter, J.; Engels, M.; Krüger, P.; Jacoby, E.; Wollmer, A. Targeted Molecular Dynamics Simulation of Conformational Change-Application to the T ↔ R Transition in Insulin. *Mol. Simul.* **1993**, *10*, 291−308.

(10) Chang, S. G.; Choi, K. D.; Jang, S. H.; Shin, H. C. Role Of Disulfide Bonds in the Structure and Activity of Human Insulin. *Mol. Cells* **2003**, *16*, 323−330.

(11) Mark, A. E.; Berendsen, H. J. C.; van Gunsteren, W. F. Conformational Flexibility of Aqueous Monomeric and Dimeric Insulin: A Molecular Dynamics Study. *Biochemistry* **1991**, *30*, 10866−10872.

(12) Cheng, Y.-K.; Rossky, P. J. The Effect of Vicinal Polar and Charged Groups on Hydrophobic Hydration. *Biopolymers* **1999**, *50*, 742−50.

(13) Chai, C. C.; Jhon, M. S. Molecular Dynamics Study on Protein and Its Water Structure at High Pressure. *Mol. Simul.* **2000**, *23*, 257−274.

(14) Badger, J.; Caspar, D. L. D. Water Structure in Cubic Insulin Crystals. *Proc. Natl. Acad. Sci. U.S.A.* **1991**, *88*, 622−626.

(15) Nandi, N.; Bhattacharyya, K.; Bagchi, B. Dielectric Relaxation and Solvation Dynamics of Water in Complex Chemical and Biological Systems. *Chem. Rev.* **2000**, *100*, 2013−2046.

(16) Bhattacharyya, K. Solvation Dynamics and Proton Transfer in Supramolecular Assemblies. *Acc. Chem. Res.* **2003**, *36*, 95−101.

(17) Pal, S. K.; Zewail, A. H. Dynamics of Water in Biological Recognition. *Chem. Rev.* **2004**, *104*, 2099−2123.

(18) Pal, S. K.; Peon, J.; Bagchi, B.; Zewail, A. H. Biological water: Femtosecond Dynamics of Macromolecular Hydration. *J. Phys. Chem. B* **2002**, *106*, 12376−12395.

(19) Das, S.; Datta, A.; Bhattacharyya, K. Deuterium Isotope Effect on 4-Aminophthalimide in Neat Water and Reverse Micelles. *J. Phys. Chem. A* **1997**, *101*, 3299−3304.

(20) Castrillón, S. R. V.; Giovambattista, N.; Aksay, I. A.; Debenedetti, P. G. Effect of Surface Polarity on the Structure and Dynamics of Water in Nanoscale Confinement. *J. Phys. Chem. B* **2009**, *113*, 1438−1446.

(21) Pizzitutti, F.; Marchi, M.; Sterpone, F.; Rossky, P. J. How Protein Surfaces Induce Anomalous Dynamics of Hydration Water. *J. Phys. Chem. B* **2007**, *111*, 7584−7590.

(22) Abbyad, P.; Shi, X.; Childs, W.; McAnaney, T. B.; Cohen, B. E.; Boxer, S. G. Measurement of Solvation Responses at Multiple Sites in a Globular Protein. *J. Phys. Chem. B* **2007**, *111*, 8269−8276.

(23) Bandyopadhyay, S.; Chakraborty, S.; Balasubramanian, S.; Bagchi, B. Sensitivity of Polar Solvation Dynamics to the Secondary Structures of Aqueous Proteins and the Role of Surface Exposure of the Probe. *J. Am. Chem. Soc.* **2005**, *127*, 4071−4075.

(24) Bandyopadhyay, S.; Chakraborty, S.; Bagchi, B. Secondary Structure Sensitivity of Hydrogen Bond Lifetime Dynamics in the Protein Hydration Layer. *J. Am. Chem. Soc.* **2005**, *127*, 16660−16667.

(25) Nandi, N.; Bagchi, B. Anomalous Dielectric Relaxation of Aqueous Protein Solutions. *J. Phys. Chem. A* **1998**, *102*, 8217−8221.

(26) Bagchi, B.; Jana, B. Solvation Dynamics in Dipolar Liquids. *Chem. Soc. Rev.* **2010**, *39*, 1936−1954.

(27) Bagchi, B. *Molecular Relaxation in Liquids*; Oxford University Press:Oxford, 2012.

(28) Adkar, B. V.; Jana, B.; Bagchi, B. Role of Water in the Enzymatic Catalysis: Study of ATP + AMP → 2ADP Conversion by Adenylate Kinase. *J. Phys. Chem. A* **2011**, *115*, 3691−3697.

(29) Hamelberg, D.; McCammon, J. A. Standard Free Energy of Releasing a Localized Water Molecule from the Binding Pockets of Proteins: Double-Decoupling Method. *J. Am. Chem. Soc.* **2004**, *126*, 7683−7689.

(30) Levy, Y.; Onuchic, J. N. Water Mediation in Protein Folding and Molecular Recognition. *Annu. Rev. Biophys. Biomol. Struct.* **2006**, 35389−415.

(31) Dennis, S.; Camacho, C. J.; Vajda, S. Continuum Electrostatic Analysis of Preferred Solvation Sites Around Proteins in Solution. *Proteins: Struct., Funct., Genet.* **2000**, *38*, 176−188.

(32) Jana, B.; Pal, S.; Bagchi, B. Hydrogen Bond Breaking Mechanism and Water Reorientational Dynamics in the Hydration Layer of Lysozyme. *J. Phys. Chem. B* **2008**, *112*, 9112−9117.

(33) Russo, D.; Hura, G.; Head-Gordon, T. Hydration Dynamics Near a Model Protein Surface. *Biophys. J.* **2004**, *86*, 1852−1862.

(34) Chandler, D. Interfaces and the Driving Force of Hydrophobic Assembly. *Nature* **2005**, *437*, 640−647.

(35) Lum, K.; Chandler, D.; Weeks, J. D. Hydrophobicity at Small and Large Length Scales. *J. Phys. Chem.* **1999**, *103*, 4570−4577.

(36) Frank, H. S.; Evans, M. W. Free Volume and Entropy in Condensed Systems 0.3. Entropy in Binary Liquid Mixtures - Partial Molal Entropy in Dilute Solutions - Structure and Thermodynamics in Aqueous Electrolytes. *J. Chem. Phys.* **1945**, *13*, 507−532.

(37) Pratt, L. R.; Chandler, D. Theory of Hydrophobic Effect. *J. Chem. Phys.* **1977**, *67*, 3683−3704.

(38) Blokzijl, W.; Engberts, J. B. F. N. Hydrophobic Effects. Opinions and Facts. *Angew. Chem., Int. Ed. Engl.* **1993**, *32*, 1545−1579.

(39) Cheng, Y. K.; Rossky, P. J. Surface Topography Dependence of Biomolecular Hydrophobic Hydration. *Nature* **1998**, *392*, 696−699.

(40) Cheng, Y. K.; Sheu, W. S.; Rossky, P. J. Hydrophobic Hydration of Amphipathic Peptides. *Biophys. J.* **1999**, 1734−1743.

(41) Cheng, Y. K.; Rossky, P. J. The Effect Of Vicinal Polar and Charged Groups on Hydrophobic Hydration. *Biopolymers* **1999**, *50*, 742−750.

(42) Meyts, P. D. Insulin and Its Receptor: Structure, Function and Evolution. *Bioessays* **2004**, *26*, 1351−1362.

(43) Gursky, O.; Li, Y.; J. Badger, J.; Caspar, D. L. Monovalent Cation Binding to Cubic Insulin Crystals. *Biophys. J.* **1992**, *61*, 604−611.

(44) Berendsen, H. J. C.; Grigera, J. R.; Straatsma, T. P. The Missing Term in Effective Pair Potentials. *J. Phys. Chem.* **1987**, *89*, 6269−6271.

(45) Hoover, W. G. Canonical Dynamics: Equilibrium Phase-Space Distributions. *Phys. Rev. A.* **1985**, *31*, 1695−1697.

(46) Nose, S. A. Unified Formulation of the Constant Temperature Molecular Dynamics Methods. *J. Chem. Phys.* **1984**, *81*, 511−19.

(47) Parinello, M.; Rahman, A. Polymorphic Transitions in Single Crystals: A New Molecular Dynamics Method. *J. Appl. Phys.* **1981**, *52*, 7182−7190.

(48) Darden, T.; York, D.; Pedersen, L. Particle Mesh Ewald: An N log(N) Method for Ewald Sums in Large Systems. *J. Chem. Phys.* **1993**, *98*, 10089−92.

(49) Frenkel, D.; Smit, B. *Understanding Molecular Simulation: From Algorithms to Applications*, 2nd ed.; Academic Press: San Diego, CA, 2002.
(50) Bandyopadhyay, S.; Chakraborty, S.; Balasubramanian, S.; Pal, S.; Bagchi, B. Atomistic Simulation Study of the Coupled Motion of Amino Acid Residues and Water Molecules around Protein HP-36: Fluctuations at and around the Active Sites. *J. Phys. Chem. B* **2004**, *108*, 12608−12616.
(51) Roy, S.; Bagchi, B. Solvation Dynamics of Tryptophan in Water-Dimethyl Sulfoxide Binary Mixture: In Search of Molecular Origin of Composition Dependent Multiple Anomalies. *J. Chem. Phys.* **2013**, *139*, 034308/1−10.
(52) Roy, S.; Bagchi, B. Free Energy Barriers for Escape of Water Molecules from Protein Hydration Layer. *J. Phys. Chem. B* **2012**, *116*, 2958−2968.
(53) Balasubramanian, S.; Bandyopadhyay, S.; Pal, S.; Bagchi, B. Dynamics of Water at the Interface of a Small Protein, Enterotoxin. *Curr. Sci.* **2003**, *85*, 1571−1578.
(54) Chandra, A.; Tuckerman, M.; Marx, D. Connecting Solvation Shell Structure to Proton Transport Kinetics in Hydrogen-Bonded Networks via Population Correlation Functions. *Phys. Rev. Lett.* **2007**, *99*, 145901/1−4.
(55) Chandra, A. Structure and Dynamics of Hydrogen Bonds in Liquid Water and Aqueous Solutions. *Proc. Indian Natl. Sci. Acad.* **2003**, *69*, 49−59.
(56) Rapaport, D. Hydrogen Bonds in Water: Network Organization and Lifetimes. *Mol. Phys.* **1983**, *50*, 1151−1162.
(57) Luzar, A.; Chandler, D. Hydrogen-bond Kinetics in Liquid Water. *Nature (London)* **1996**, *379*, 55−57.
(58) Chandra, A. Effects of Ion Atmosphere on Hydrogen-Bond Dynamics in Aqueous Electrolyte Solutions. *Phys. Rev. Lett.* **2000**, *85*, 768−771.
(59) Xu, H.; Berne, B. J. Hydrogen-Bond Kinetics in the Solvation Shell of a Polypeptide. *J. Phys. Chem. B* **2001**, *105*, 11929−32.
(60) Badger, J. Multiple Hydration Layers in Cubic Insulin Crystals. *Biophys. J.* **1993**, *65*, 1656−1659.